ChemComm

COMMUNICATION

View Article Online
View Journal

Cite this: DOI: 10.1039/d1cc00118c

Received 8th January 2021,
Accepted 23rd August 2021

DOI: 10.1039/d1cc00118c

rsc.li/chemcomm

Cell-specific activation of gemcitabine by endogenous H_2S stimulation and tracking through simultaneous fluorescence turn-on†

Mrinmoy Maiti,‡[a] Shin A. Yoon,‡[b] Yujin Cha,[b] K. K. Athul,[c] Sankarprasad Bhuniya *[c] and Min Hee Lee *[b]

The endogenous H_2S-driven theranostic H_2S-Gem has been invented. The theranostic prodrug H_2S-Gem is selectively activated in cancer cells, releasing active gemcitabine with a simultaneous fluorescence turn-on. H_2S-Gem selectively inhibited cancer cell growth compared to the mother chemotherapeutic gemcitabine. Overall, it is a unique protocol for tracking and transporting chemotherapeutic agents to tumor areas without the guidance of tumor-directive ligands.

Cancer is a major disease burden that threatens people's lives worldwide, and the majority of cancer-related deaths are due to metastasis of the original tumor.[1] Current treatment options at the diagnosis level are multimodal and include chemotherapy, radiotherapy, and surgical resection or combination therapy. Although chemotherapy and radiotherapy show significant treatment modalities for cancer, they are still hindered by acute side effects on neighboring healthy cells/tissues due to their high toxicity and non-selectivity.[2–9] Indeed, cancer cells are resistant to radiotherapy and chemotherapy.[10,11] Therefore, new concepts are highly desirable for the precise diagnosis and effective treatment of cancer. One such type of modality is theranostics, a modern technology with a bi-functional system that serves as both a therapy and the diagnosis. This technique is particularly interesting as it provides real-time information on cancer therapy. By using this method, different cancer targeting molecules, anticancer drugs, and fluorophores are covalently conjugated through chemical reactions that provide biodistributed chemotherapeutic and therapeutic interventions through fluorescence imaging. Several endogenous stimulators have been considered to develop such an all in one system.[12]

Recently, it has been observed that endogenous H_2S is produced to a large extent in several cancer cells, increasing cell proliferation activity.[13] Mostly, cystathionine β-synthase (CBS) and cystathionine γ-lyase are the major enzymes responsible for producing endogenous H_2S in cancer cells.[13] Recently, by considering endogenous H_2S as a stimulator a few theranostic molecules[14] have been developed including inhibition of cancer cell growth selectively in cancer cells. Thus, we believe that endogenous H_2S can be a suitable stimulator for transporting chemotherapeutics to the desired area with maximum clinical benefits without causing adverse side effects.

In the present work, gemcitabine is linked through a labile secondary amine bond with an inactive form of coumarin (Scheme 1). Gemcitabine was used as a model drug because it treats various cancers and has serious adverse effects.[15,16] In addition, this strategy may increase the half-life of gemcitabine. Also, as gemcitabine is a non-fluorescent therapeutic, tracking with a fluorescent reporter is important. The endogenous H_2S induced reduction of N_3 to amine, triggering a secondary amine bond cleavage that releases the gemcitabine *via* a self-immolative pathway is proposed in Scheme 1. In this event, the reduction of an azide group to an electron rich NH_2 group in coumarin will increase the fluorescence intensity. The detail of

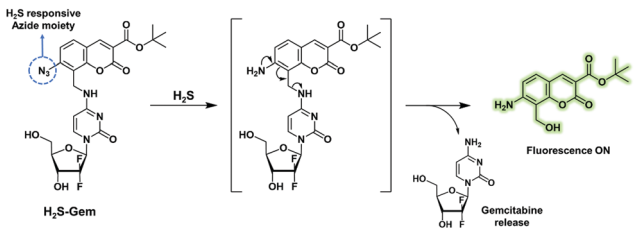

Scheme 1 Activation mechanism of **H_2S-Gem** for H_2S.

[a] Department of Science, School of Engineering, Amrita Vishwa Vidyapeetham, Coimbatore, 641112, India
[b] Department of Chemistry, Sookmyung Women's University, Seoul 04310, Korea. E-mail: minheelee@sookmyung.ac.kr
[c] Centre for Interdisciplinary Science, JIS Institute of Advanced Studies and Research, JIS University, Salt Lake, Kolkata, 700091, India. E-mail: spbhuniya@jisiasr.org

† Electronic supplementary information (ESI) available. See DOI: 10.1039/d1cc00118c

‡ These authors equally contributed to this work.

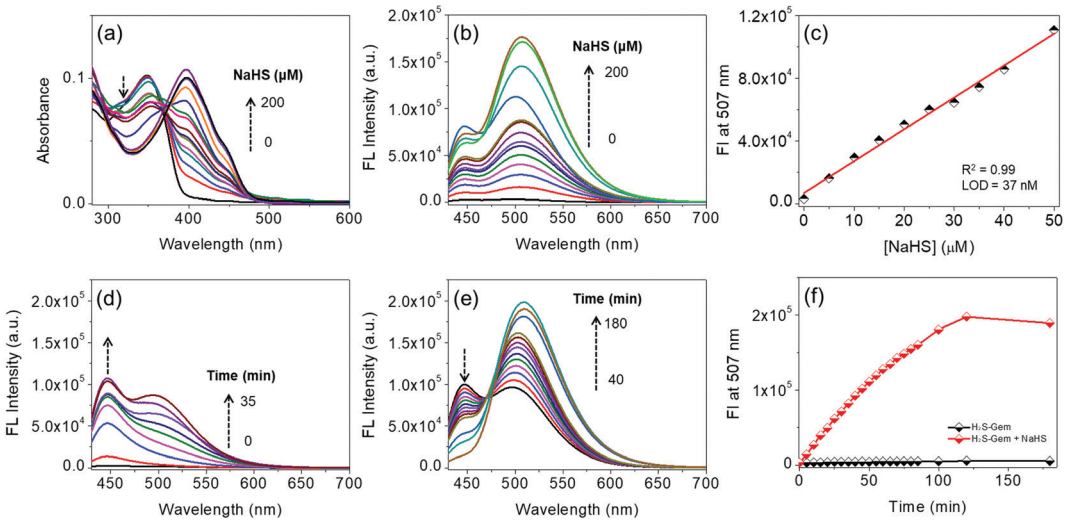

Fig. 1 (a) UV-absorption and (b) fluorescence spectra of **H_2S-Gem** (5 μM) for various concentrations of NaHS (0–200 μM) after 1 h incubation at 37 °C. (c) Plot of fluorescence intensity at 507 nm in the presence of NaHS (0–50 μM). Fluorescence changes of **H_2S-Gem** (5 μM) with NaHS (200 μM) at different time intervals (d) 0–35 min and (e) 40–180 min. (f) Time-dependent fluorescence changes of **H_2S-Gem** (5 μM) in the absence (black) and presence (red) of NaHS (200 μM). All data were obtained in a PBS (10 mM, pH 7.4) solution containing 1% (v/v) of DMSO using an excitation wavelength of 410 nm.

the synthetic route for **H_2S-Gem** is available in the ESI† including spectroscopic analysis data (Scheme S1 and Fig. S1–S22).

To continue to prove our concept, initially, we have examined the exogenous H_2S response of **H_2S-Gem** by recording UV-absorption changes in H_2S (NaHS) treated **H_2S-Gem** under physiological conditions (Fig. 1a and Fig. S23, ESI†). We observed that the UV-absorption of **H_2S-Gem** showed a bathochromic shift from 350 nm to 410 nm with increasing doses of H_2S (Fig. 1a). Similarly, in the H_2S dose-dependent titration, we observed the fluorescence intensity at 507 nm increased compared to the shoulder peak at 450 nm (Fig. 1b). The fluorescence increment with different doses of H_2S showed perfect linearity (R^2 = 0.99) with a low detection limit (LOD) of 37 nM (Fig. 1c).[17] The time-course study initially (0–35 min) showed increments in fluorescence at 450 nm and 507 nm (Fig. 1d); however, as time progressed (after 35 min), it showed a ratiometric fluorescence change at 450 nm and 507 nm (Fig. 1e). The fluorescence intensity reached saturation within 120 min (Fig. 1f).

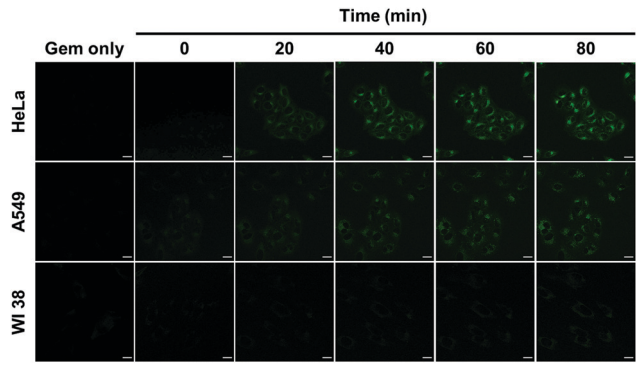

Fig. 2 Time-dependent cancer cell labeling. Cells were administered with **H_2S-Gem** (15 μM) for 0–80 min. Emission collected in the 505–600 nm region with the excitation wavelength set at 405 nm. Scale bar: 20 μm.

Further, we tested the chemoselectivity between **H_2S-Gem** and H_2S in comparison with other biologically relevant analytes such as various metal ions, ROS, Cys, Hcy, GSH, $NaNO_2$, Na_2CO_3 and ascorbic acid. It was noticed that **H_2S-Gem** remains inactive in altering the fluorescence signal in all cases (Fig. S24, ESI†). In addition, the kinetic stack plot of **H_2S-Gem** with 1 mM of various thiols such as Cys, Hcy, GSH and NaHS firmly showed that NaHS dominantly increases the fluorescence of **H_2S-Gem**, unlike the other thiols (Fig. S25, ESI†). These results proved that **H_2S-Gem** is chemoselective towards H_2S. Moreover, the pH-dependent chemoselective reaction between **H_2S-Gem** and H_2S has been investigated. The result in Fig. S26 (ESI†) indicated that within a biologically relevant pH, **H_2S-Gem** reacted with H_2S. Nonetheless, the reactivity between **H_2S-Gem** and H_2S is highest in the pH 6 to 8 range.

Next, the H_2S-driven structural changes in **H_2S-Gem** that cause the fluorescence signal were confirmed using mass analysis of H_2S pretreated **H_2S-Gem**. It was observed that mass peaks for gemcitabine and the fluorophore appeared (Fig. S27, ESI†).

After confirming the H_2S triggered gemcitabine release, we investigated the *in vitro* cell labeling to determine the cell-specific gemcitabine release from **H_2S-Gem**. In a time-dependent fluorescence study, we observed that the extent of fluorescence labeling in a couple of cancer cell lines (HeLa and A549) increased with the incubation period (Fig. 2). It indicated that both cervical cancer cells (HeLa) and adenocarcinoma human alveolar basal epithelial cells (A549) have sufficient endogenous H_2S that released active gemcitabine from **H_2S-Gem**. On the contrary, **H_2S-Gem** pretreated human normal fibroblast WI38 cells did not show such fluorescence. Whereas

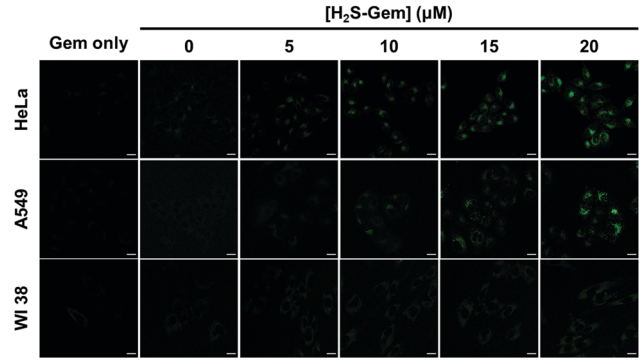

Fig. 3 Dose-dependent cancer cell labelling. Cells were incubated with **H_2S-Gem** (0–20 μM) for 60 min prior to imaging using a confocal microscope. Emission collected in the 505–600 nm region with the excitation wavelength set at 405 nm. Scale bar: 20 μm.

WI38 cells treated with exogenous H_2S were labeled with green fluorescence (Fig. S28, ESI†). This implied that the theranostic **H_2S-Gem** entered into the WI38 cells, but due to insufficient endogenous H_2S it failed to activate the **H_2S-Gem** to provide fluorescence images.

Further, in a concentration-dependent study, we observed that the extent of fluorescence labeling in cancer cells (HeLa and A549 cells) increased with the dose of **H_2S-Gem** (Fig. 3); however, normal fibroblast cells (WI38 cells) did not show any fluorescence under identical conditions. Moreover, the fluorescence intensity also increased according to the concentration of NaHS (Fig. S29, ESI†). This indicated that the endogenous H_2S level in cancer cells is higher than that in normal cells.

Next, we clarified whether such fluorescence images in the **H_2S-Gem** pretreated cancer cells were due to endogenous H_2S or other thiol species. Thus, we recorded fluorescence images of living cells by altering the formation of endogenous H_2S in living cells. In Fig. 4 and Fig. S30 (ESI†), we noticed that while cells were pretreated with exogenous H_2S (NaHS), the fluorescence images in the green channel increased because of **H_2S-Gem**. Further, the exogenous addition of a substrate (cysteine) produces excess H_2S,[13] which is well reflected in the fluorescence images by an increment in fluorescence intensity. On the other hand, cystathionine β-synthase and cystathionine γ-lyase inhibitor *i.e.* aminooxyacetic acid (AOAA) and *N*-propargyl glycine (PAG)[13,18] pretreated cancer cells showed a decreased fluorescence signal in the green channel. This suggested that inhibition of the H_2S producing enzymes reduces the release of gemcitabine from the theranostic **H_2S-Gem** and the formation of the fluorophore.

Finally, we evaluated the anticancer activity of the theranostic **H_2S-Gem** using both the dose- and time-dependent MTT assay methods. We observed that about 50% of the cell growth was inhibited upon incubation (48–72 h) with 5 μM of **H_2S-Gem** with A549 and HeLa cells, respectively (Fig. 5a, b and Fig. S31a, ESI†). Concentrations of up to 60 μM of **H_2S-Gem** failed to show considerable cell growth inhibition in normal human fibroblast WI38 cells (Fig. 5c and Fig. S31a, ESI†). While the theranostic **H_2S-Gem** has shown cancer cell specific activation of gemcitabine, gemcitabine alone has shown nonspecific cell growth inhibition irrespective of cancer cells and normal WI38 cells (Fig. S31b, ESI†). Additionally, the anti-proliferative activity of **H_2S-Gem** was monitored in NaHS and PAG-treated HeLa cells. Compared to the untreated HeLa cells, for **H_2S-Gem**, the NaHS-treated cells showed a decreased cell viability whereas the PAG-treated cells exhibited an increased cell viability (Fig. S32, ESI†). Additionally, the high cell viability of the released fluorophore pretreated HeLa cells indicates that the growth inhibition of **H_2S-Gem** incubated cancer cells is because of the release of nascent gemcitabine from **H_2S-Gem** (Fig. S33, ESI†). Such specific cell growth inhibition toward cancer cells indicated that endogenous H_2S in cancer cells allows **H_2S-Gem** to release active chemotherapeutic gemcitabine. In contrast,

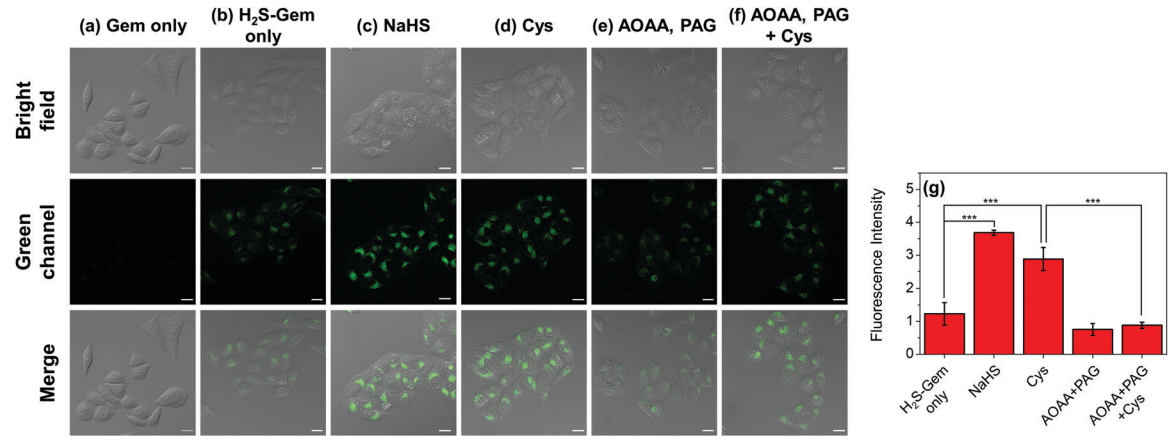

Fig. 4 Confocal microscopy images of **H_2S-Gem** in HeLa cells. Cells were incubated with (a) gemcitabine (15 μM) and (b) **H_2S-Gem** (15 μM) for 1 h, respectively. (c) Cells were pretreated with **H_2S-Gem** for 1 h then incubated with NaHS (600 μM) for 30 min. (d) Cells were pretreated with cysteine (200 μM) for 1 h then incubated with **H_2S-Gem** for 1 h. (e) Cells were pretreated with AOAA/PAG (2 mM) for 1 h then incubated with **H_2S-Gem** for 1 h. (f) Cells were pretreated with AOAA/PAG (2 mM) and cysteine (200 μM) for 1 h, respectively, then incubated with **H_2S-Gem** for 1 h. All images were obtained using a laser with an excitation wavelength of 405 nm and a band-path filter of 505–600 nm. Scale bar: 20 μm. (g) Quantification of the fluorescence intensities from each cell. Error bars indicate the standard deviation (SD). Asterisks indicate statistically significant changes (***$P \leq 0.001$).

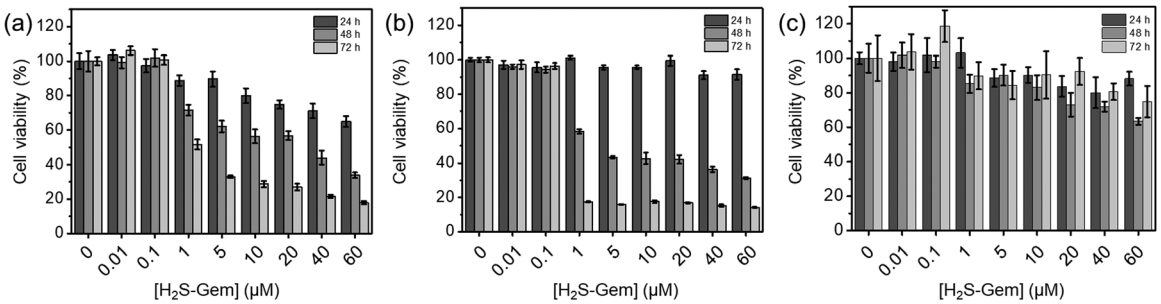

Fig. 5 MTT assay of **H_2S-Gem** for 24, 48 and 72 h in (a) HeLa, (b) A549 and (c) WI38 cells. Error bars indicate SD, n = 5.

insufficient endogenous H_2S formation in WI38 cells disfavors **H_2S-Gem** to show a considerable extent of anti-proliferative activity.

In conclusion, we demonstrated the endogenous H_2S stimulated theranostic **H_2S-Gem** for selectively ending the progression of cancer *via* activation of chemotherapeutic gemcitabine. The theranostic prodrug **H_2S-Gem** constituted of a combination of coumarin and gemcitabine. It showed UV-absorption at 400 nm and emission at 505 nm in the presence of exogenous H_2S. This theranostic **H_2S-Gem** was even activated in the presence of a minimal quantity (37 nM) of H_2S. The gemcitabine release process is highly selective toward H_2S, and such a specific activation allows gemcitabine release exclusively in cancer cells. *In vitro* cellular images indicated that the endogenous H_2S level in cancer cells is relatively high compared to that in the normal WI38 cells. The inhibition assay study indicated that cystathionine β-synthase and cystathionine γ-lyase are sources of H_2S formation in cancer cells. It showed selective antiproliferative activity exclusively in the cancer cells (HeLa and A549) over the human normal fibroblast cells (WI38). All of these facts advocated that it is a unique strategy for releasing cargo and selectively tracking therapeutic events in cancer cells without the support of any tumor/cancer cell-specific ligands.

This research was supported by the National Research Foundation of Korea (NRF) grant funded by the Korea government (MSIT) (2021R1F1A1045790). Also, this work is supported by the SERB, India (Grant No. CRG/2019/002068, SB), CSIR-India (Grant No. 02(0386)19/EMR II, SB), and the DST (INT/RUS/RFBR/392, SB).

Conflicts of interest

There are no conflicts to declare.

Notes and references

1 R. L. Siegel, K. D. Miller and A. Jemal, *Ca-Cancer J. Clin.*, 2019, **69**, 7–34.
2 J. H. Atkins and L. J. Gershell, *Nat. Rev. Cancer*, 2002, **2**, 645–646.
3 D. J. Irvine, *Nat. Mater.*, 2011, **10**, 342–343.
4 J. A. Hubbell and R. Langer, *Nat. Mater.*, 2013, **12**, 963–966.
5 S. Mura, J. Nicolas and P. Couvreur, *Nat. Mater.*, 2013, **12**, 991–1003.
6 R. Mahato, W. Tai and K. Cheng, *Adv. Drug Delivery Rev.*, 2011, **63**, 659–670.
7 S. Zhang, K. H. Chan, R. K. Prud'Homme and A. Link, *Mol. Pharmaceutics*, 2012, **9**, 2228–2236.
8 E. Kim, D. Kim, H. Jung, J. Lee, S. Paul, N. Selvapalam, Y. Yang, N. Lim, C. G. Park and K. Kim, *Angew. Chem., Int. Ed.*, 2010, **49**, 4405–4408.
9 G. Cafeo, G. Carbotti, A. Cuzzola, M. Fabbi, S. Ferrini, F. H. Kohnke, G. Papanikolaou, M. R. Plutino, C. Rosano and A. J. P. White, *J. Am. Chem. Soc.*, 2013, **135**, 2544–2551.
10 C. Sawyers, *Nature*, 2004, **432**, 294–297.
11 I. Brigger, C. Dubernet and P. Couvreur, *Adv. Drug Delivery Rev.*, 2012, **64**, 24–36.
12 (*a*) Y. Zhou, M. Maiti, A. Sharma, L. Yu, X. W. Lv, J. Shin, M. Won, J. Han, A. Podder, K. N. Bobba, S. Bhuniya and J. S. Kim, *J. Controlled Release*, 2018, **288**, 14–22; (*b*) A. Sharma, M.-G. Lee, H. Shi, M. Won, J. F. Arambula, J. L. Sessler, J. Y. Lee, S.-G. Chi and J. S. Kim, *Chem*, 2018, **4**, 2370–2383; (*c*) S. Barman, S. K. Mukhopadhyay, S. Biswas, S. Nandi, M. Gangopadhyay, S. Dey, A. Anoop and N. D. Pradeep Singh, *Angew. Chem.*, 2016, **128**, 4266–4270; (*d*) S. Maiti, N. Park, J. H. Han, H. M. Jeon, J. H. Lee, S. Bhuniya, C. Kang and J. S. Kim, *J. Am. Chem. Soc.*, 2013, **135**, 4567–4572; (*e*) R. Kumar, E.-J. Kim, J. Han, H. Lee, W. S. Shin, H. M. Kim, S. Bhuniya, J. S. Kim and K. S. Hong, *Biomaterials*, 2016, **104**, 119–128; (*f*) F. Kong, Z. Liang, D. Luan, X. Liu, K. Xu and B. A. Tang, *Anal. Chem.*, 2016, **88**, 6450–6456; (*g*) T. Kim, H. M. Jeon, H. T. Le, T. W. Kim, C. Kang and J. S. Kim, *Chem. Commun.*, 2014, **50**, 7690–7693; (*h*) P. Liu, D. Yan, P. Zhang, F. Zeng, B. Li and S. A. Wu, *Chem. Commun.*, 2015, **51**, 9567–9570; (*i*) D. Dutta, S. M. Alex, K. N. Bobba, K. K. Maiti and S. Bhuniya, *ACS Appl. Mater. Interfaces*, 2016, **8**, 33430–33438.
13 C. Szabo, C. Coletta, C. Chao, K. Módis, B. Szczesny, A. Papapetropoulos and M. R. Hellmich, *Proc. Natl. Acad. Sci. U. S. A.*, 2013, **110**, 12474–12479.
14 (*a*) H. Zhang, X. Kong, Y. Tang and W. Lin, *ACS Appl. Mater. Interfaces*, 2016, **8**, 16227–16239; (*b*) D. Zheng, Z. Gao, T. Xu, C. Liang, Y. Shi, L. Wang and Z. Yang, *Nanoscale*, 2018, **10**, 21459–21465; (*c*) K. N. Bobba, G. Saranya, P. T. Sujai, M. M. Joseph, N. Velusamy, A. Podder, K. K. Maiti and S. Bhuniya, *ACS Appl. Bio Mater.*, 2019, **2**, 1322–1330; (*d*) K. N. Bobba, A. Binoy, S. Koo, A. Podder, N. Mishra, J. S. Kim and S. Bhuniya, *Chem. Commun.*, 2019, **55**, 6429–6432; (*e*) B. Shi, N. Ren, L. Gu, G. Xu, R. Wang, T. Zhu, Y. Zhu, C. Fan, C. Zhao and H. Tian, *Angew. Chem., Int. Ed.*, 2019, **58**, 16826–16830.
15 A. Henthorn and M. D. Pluth, *J. Am. Chem. Soc.*, 2015, **137**, 15330–15336.
16 H. C. Zhu, C. X. Liang, X. X. Cai, H. M. Zhang, C. Y. Liu, P. Jia, Z. L. Li, Y. M. Yu, X. Zhang, W. L. Sheng and B. C. Zhu, *Anal. Chem.*, 2019, **92**, 1883–1889.
17 S. Y. Park, W. Kim, S. H. Park, J. Han, J. Lee, C. Kang and M. H. Lee, *Chem. Commun.*, 2017, **53**, 4457–4460.
18 N. Velusamy, A. Binoy, K. N. Bobba, D. Nedungadi, N. Mishra and S. Bhuniya, *Chem. Commun.*, 2017, **53**, 8802.

